

Strength Degradation of Glass Impacted with Sharp Particles: II, Tempered Surfaces

B. R. LAWN* and D. B. MARSHALL

Department of Applied Physics, School of Physics, The University of New South Wales, New South Wales 2033, Australia

S. M. WIEDERHORN*

Fracture and Deformation Division, National Bureau of Standards, Washington, D.C. 20234

The analysis of strength degradation in the preceding paper is here extended to tempered surfaces. Addition of a surface compression term to the indentation fracture equations leads to simply modified degradation relations. Impact energy is again identified as the important service variable in degradation. Comparative strength tests on thermally tempered and annealed glass disks after impactation with SiC particles confirm the predicted energy dependence of strength loss. The results indicate that surface-strengthening processes can be just as effective in improving resistance to strength degradation as can increasing toughness. However, improvements in surface erosion resistance are relatively insignificant.

I. Introduction

CHARACTERIZING the strength of ceramics for structural design purposes involves two major questions: how can strength be predicted and how can it be improved? In Part I¹ the first of these questions was considered. There it was concluded that it is material parameters which largely control the resistance to prospective strength loss in ordinary annealed surfaces: high toughness, and, to a lesser extent, low hardness, were the design goals.

In this part of the study the second question is addressed. Since choice of material for any given application may be limited by the necessity to meet other stringent design specifications (e.g. high thermal shock resistance or optical transparency in a certain wavelength region), techniques for improving the resistance to strength degradation of a specified materials system are of particular interest. With many ceramics limited benefits can be gained by appropriate refinements in microstructure, mainly through an increase in the toughness. Any attendant refinement in size or density of flaws is of little additional value, since sharp indenters are capable of acting as their own sources of crack nucleation: the capability of a single in-service contact event for degrading the strength to a level independent of initial flaw characteristics has been discussed.¹ For the same reason, etching of glass components to remove surface flaws can be futile unless an effective method of protective coating is available. The most practical route to improved strength, especially in glasses, is to put the surfaces into residual compression.²

The aim of the present work was to extend the sharp-particle impact analysis of Part I to tempered surfaces. The foundation for such an extension was laid in a study of the strength characteristics of thermally tempered glass plates degraded by static contact with Vickers diamond pyramid indenters.³ The procedure was the same as in Part I, with recourse to Ref. 3 for modified strength and indentation fracture equations incorporating an appropriate residual compression term. The choice of thermally tempered glass as a model surface-strengthened system does not detract from the generality of the basic approach: several alternative physical and chemical tempering processes now exist for achieving surface compression² and, notwithstanding certain limitations (to be pointed out later), should be amenable to at least a first-approximation analysis in terms of the degradation equations derived herein.

II. Modification of Strength/Velocity Characteristic

In setting up a theory of strength degradation for tempered surfaces it is necessary to specify the residual stresses. The important components are those parallel to the surface. Within the surface itself these stresses are strongly compressive, but below the surface they necessarily become tensile to satisfy the requirement of zero net section force: for instance, for a thermally tempered glass plate the section profile of stress is closely parabolic, with the inner tension approximately one-half the outer compression.² The compressive stresses may also vary over the surface, although such variations are relatively slight in plates with large surface area and small thickness.⁴ The principal stress along the surface normal is generally of only secondary importance, diminishing to zero at the outer layers. In the present work the effects of stress gradients are considered to be negligible, so that a single surface-compression parameter, σ_R , suffices to specify the intensity of the residual field. Such an approximation is reasonable if the prospective target area is small compared to the total surface area of a specimen and if the depth of indentation cracks is small compared to the thickness of the compression zone.

Theoretical development is in three steps, as in Part I. First, the maximum impulsive load, P_m , delivered to the target surface by the impacting particle of velocity v must be determined. Section II(1) of the preceding paper shows that the work of penetration of a sharp, rigid particle of specified impact parameters is governed exclusively by the plastic properties of the target surface, i.e. by the hardness H . Thus for a particle of mass m , characteristic included angle 2ψ , and indentation geometry factor Λ (as defined by $P/\Lambda\pi a^2 = H$, with P the indentation load and a some characteristic dimension of the impression), the relevant equation is

$$P_m = (9\Lambda\pi H \tan^2 \psi)^{1/3} U_K^{2/3} = (2,25\Lambda\pi H m \tan^2 \psi)^{1/3} v^{4/3} \quad (1)$$

as before,¹ but with H now pertaining to the tempered surface. With thermally tempered glass plates the effect of the strengthening treatment on H is minimal.³

The next step is to specify appropriate indentation fracture relations. The downward-penetrating median cracks primarily responsible for strength degradation are inhibited in their evolution by the surface compression,⁵ so σ_R must enter the formulation. For the initiation stage of median cracking⁶ it can be shown (Appendix) that the threshold relation (Eq. (8) in Part I) modifies to

$$P_c = [\alpha_p / (1 - \sigma_R / \sigma_m)^3] K_c^4 / H^3 = \alpha_p' K_c^4 / H^3 \quad (2)$$

with $\alpha_p' (> \alpha_p)$ a modified indentation geometry factor, σ_m (αH) the peak tensile stress at the nucleation center in the elastic/plastic field, and K_c the toughness. As with the hardness, K_c is unchanged by the thermal tempering process.³ For the propagation stage of median cracking the Griffith/Irwin fracture mechanics expression (Eq. (9) in Part I) relating median crack size D to load modifies to³

$$P/D^{3/2} = \beta_p [K_c + \sigma_R (\pi \Omega D)^{1/2}] \quad (P > P_c) \quad (3)$$

with the geometrical factors β_p and Ω as before.

With a suitable calibration of the α and β factors in Eqs. (2) and (3), along with the approximation $\Omega = 4/\pi^2$ for ideal penny-like medians, equating P_c and P to P_m in Eq. (1) yields a threshold impact energy U_{Kc} and crack-size function $D(U_K)$ ($U_K > U_{Kc}$). That is, in principal the scale of cracking may be predetermined for any

Received March 10, 1978.

Supported at the University of New South Wales by the Australian Research Grants Committee and at The National Bureau of Standards by the U.S. Office of Naval Research, Metallurgy and Ceramics Program.

*Member, the American Ceramic Society.

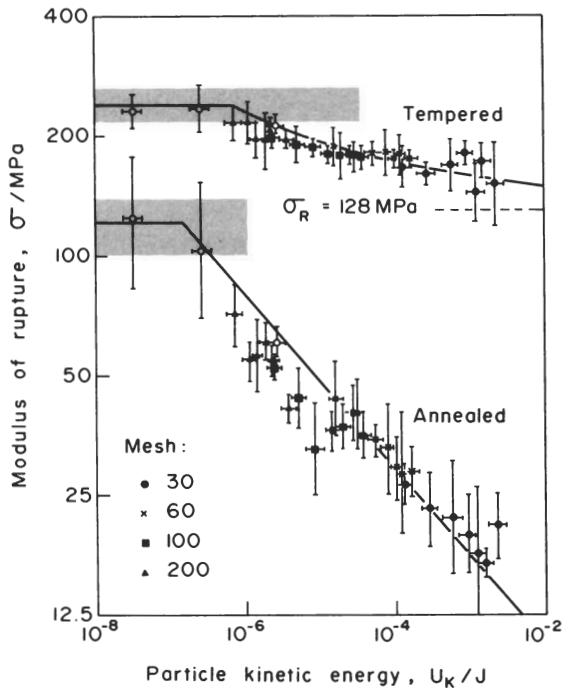


Fig. 1. Strength degradation of tempered and annealed crown glass disks impacted with SiC grit particles (open symbols designate free-fall data). Shading designates standard deviation limits of strengths for unimpacted disks (as-received).

given impact parameters and tempered surface. As with untempered glass surfaces U_{Kc} is often small enough that the existence of a threshold does not become evident in strength degradation data, in which case $U_{Kc} \approx 0$ (Ref. 1) is a reasonable approximation.

In addition to the strength-impairing median cracks there are the lateral cracks which spread sideways from the deformation zone on unloading and cause surface chipping.⁷ These cracks are not expected to be so strongly affected by the residual field associated with the tempering, since the near-zero component of stress along the normal to both free surface and crack plane contributes little to the elastic/plastic force field responsible for driving the fracture.

Finally, the standard strength relation (Eq. (10) in Part I) is modified by the surface compression to³

$$\sigma = K_c / (\pi c_f)^{1/2} + \sigma_R \quad (4)$$

with c_f the effective length of the dominant flaw. A "cutoff" particle energy U_K^* is defined such that¹

$$c_f = c_{f0} \quad (U_K < U_K^*) \quad (5a)$$

$$c_f = \Omega D \quad (U_K > U_K^*) \quad (5b)$$

where c_{f0} is the characteristic size of preexisting flaws.

Eliminating crack length and indentation load from these equations then gives the strength degradation characteristics

$$\sigma(1 - \sigma_R/\sigma) = K_c / (\pi c_{f0})^{1/2} \quad (U_K < U_K^*) \quad (6a)$$

$$\sigma(1 - \sigma_R/\sigma)^{4/3} = [(1/9\pi^{5.5})^{1/9} (\beta_p^3/\Lambda \tan^2 \psi)^{1/9} / (K_c^{4/3}/\Omega^{1/2} H^{1/9})] U_K^{-2/9} \quad (U_K > U_K^*) \quad (6b)$$

Note that these relations reduce to Eq. (12) in Part I in the limit of $\sigma_R = 0$ and that $\sigma > \sigma_R$ always (provided that the approximation of zero stress gradients remains reasonably well satisfied).

III. Experimental Procedure

(1) Impact Apparatus and Contact Parameters

The procedure used to impact the sharp particles onto the target surface was exactly as described in Part I; SiC grit of mesh sizes 30,

60, 100, and 200 (See Table I of Part I) were accelerated in an air stream to projectile velocities of up to 120 ms⁻¹. Glass again constituted the target material, but this time crown glass disks (50 mm in diam. and 3 mm thick), as used in a previous study,³ replaced the laths; here commercial availability in the thermally tempered state was the prime factor in selection of a suitable test specimen. After impactation the target area was covered with mineral oil to minimize kinetic effects in the subsequent strength tests. Strength was measured in a concentric ring-on-ring flexure arrangement (inner support radius 8.0 mm, outer support radius 19.8 mm) with the central impacted area of the disk placed on the tension side³; apart from eliminating premature edge failures, this method had the advantage of producing rupture under essentially biaxial stress conditions, in keeping with the biaxial state of the residual stress field. In addition to the strength tests, some of the disks were weighed before and after impactation to determine the level of surface erosion.

The essential strength degradation parameters for the glass surfaces were obtained in the usual way from calibration tests with a Vickers pyramid indenter in conjunction with flexure tests.³ In their as-received state the disks had a surface compression of $\sigma_R = (128 \pm 15)$ MPa. Some disks were annealed to produce specimens free of residual stress, $\sigma_R = (0 \pm 2)$ MPa, for control tests. Base levels of strength for unimpacted disks were measured as $\sigma = (237 \pm 22)$ MPa (tempered) and $\sigma = (121 \pm 21)$ MPa (annealed) (mean \pm standard deviation, 20 disks each). In the approximation of ideal penny-like geometry for the median cracks, i.e. $\Omega = 4/\pi^2$, the indentation/strength data for the annealed disks gave an effective toughness³ $K_c = (0.47 \pm 0.07)$ MPa m^{1/2}. From the same data the indentation fracture coefficient $\beta_p = 17.5 \pm 3.3$ was evaluated: together with $\Lambda = 2/\pi$ and $\psi = 74^\circ$ for Vickers indentations (referred to impression half-diagonal as characteristic dimension), this gives the composite term $(\beta_p^3/\Lambda \tan^2 \psi)^{1/9} = 2.07 \pm 0.09$ for insertion into Eq. (6b). The hardness was measured at $H = (5.5 \pm 0.2)$ GPa (tempered) and $H = (5.7 \pm 0.2)$ GPa (annealed) (50 indentations each), underlying the insensitivity of hardness to surface stress.

Microscopic examination of SiC-impacted glass surfaces revealed a superficial similarity in the damage morphology for tempered and annealed disks. The pronounced surface spalling seen in Fig. 3(A) of Part I was again evident, with little apparent difference between the two surface types. This observation is consistent with the expected small influence of the residual stress field on the growth of lateral cracks (Section II). Because of the excessive chipping it was not always easy to identify a central deformation region corresponding to the plastic contact zone in individual damage patterns, but where this was possible there was no measurable difference in the scale of deformation on tempered and annealed surfaces. Again, this is consistent with the near-constancy in hardness values observed above. Most significantly, however, there was a noticeable tendency toward reduced median-crack surface traces in going from annealed to tempered surfaces, in line with the key predictions of Eqs. (2) and (3).

(2) Strength Degradation Results

Impact/strength tests were run on tempered and annealed glass disks. The kinetic energy of individual SiC particles impinging on a given disk was evaluated from the measured velocity and the estimated mass for the appropriate mesh size (Table I in Part I). At each test energy strengths were measured for four disks and a representative mean and standard deviation thereby determined. The corresponding theoretical degradation function $\sigma(U_K)$ was generated from Eq. (6) using the parameters specified in Section III(1). Theoretical prediction (solid lines) and experimental results (data points) are shown for both tempered and annealed surfaces in Fig. 1. Distinction is again made between a low-energy impact region, controlled by preexistent surface flaws, and a high-energy region, controlled by indentation cracks. There is no clear evidence for a threshold energy, suggesting that newly initiated median cracks do not exceed the size of preexistent flaws on the as-received surfaces.

It is evident from Fig. 1 that the tempering process offers the prospect of dramatic improvement in the resistance to strength degradation, at least over the particle energy range studied. Also, the idea of "universality" in the $\sigma(U_K)$ function for a given materi-

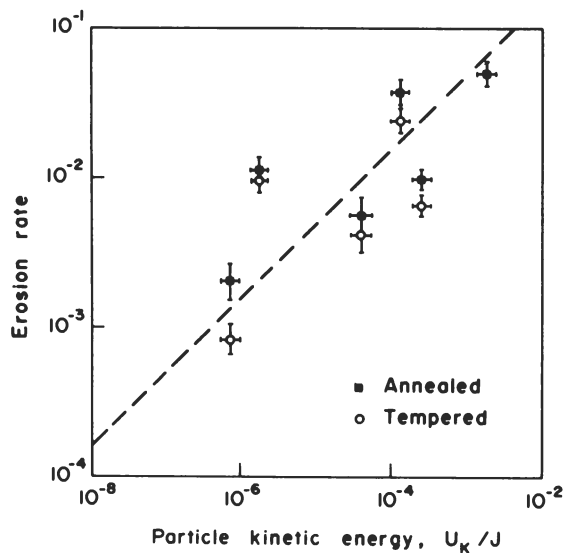


Fig. 2. Erosion of tempered and annealed crown glass disks impacted with SiC grit particles, expressed as weight material removed/weight incident abrasive.

als system alluded to in Part I clearly needs to be revised in terms of a modified $[\sigma(U_k)]_{\sigma_R}$ function to allow for the effects of surface stress.

(3) Erosion Results

Some sample erosion measurements were made on the glass disks to supplement the strength data. For each test an erosion rate was recorded in terms of weight loss of target material per weight of abrasive striking the surface. The data are presented in Fig. 2 as a function of particle kinetic energy. Even allowing for the scatter in results, typical of erosion data,⁸ there does appear to be a slight improvement in resistance to surface removal as a result of tempering. However, this improvement is far less than that evident in the strength characteristics. Moreover, the tempered disks were prone to spontaneous failure as the degree of erosion became severe, indicating that the impact-induced cracks were beginning to penetrate into the central tension zone.

IV. Discussion

The prospect of surface tempering adds a new dimension in the design of strong ceramics for particle-impact situations. Inspection of Eq. (6) shows that materials-selection requirements are unaffected by the degree of surface tempering, with high toughness of primary importance and low hardness (or, with blunt indenters, stiffness) of secondary importance.¹ The interesting conclusion to be drawn from Eq. (6) in the context of the present study is that σ_R is no less important a parameter than K_c in designing for the ultimate in strength-degradation resistance. Thus, in Fig. 1, note that the effect of tempering the glass disks is equivalent to an increase of almost an order of magnitude in toughness.

However, such implications in design must be considered in the light of underlying assumptions implicit in the analysis. Most importantly, the median cracks responsible for ensuing failure are presumed to be contained in the near-surface zone of residual compression (Section II), so that the fracture mechanics may be treated in terms of an ideal penny crack in a uniform stress field. In cases of severe surface degradation where the indentation cracks penetrate toward the inner regions of a target specimen, stress gradient effects can no longer be neglected, as manifested by the crack-geometry factor Ω in Eqs. (3), (5), and (6) becoming a diminishing function of D .^{3,9} Where the surface compression layer is characteristically thin, as in typical chemically tempered surfaces, this type of effect demands particular attention.

Another point to be considered when establishing design criteria for mechanical integrity is that high resistance to strength degrada-

tion does not necessarily imply high resistance to erosion. The comparative data presented in Section III on tempered and annealed glass show that this point is especially relevant to surface-strengthened targets. Whereas the penetrative median cracks responsible for strength loss are strongly inhibited in their growth by the large component of compressive stress parallel to the surface, the sideways-extending lateral cracks responsible for erosion are relatively unaffected by the minor component of residual stress normal to the surface. This underlines the need to have basic information on all aspects of crack evolution in the indentation event, especially in view of the geometrical variants that have been reported in different brittle materials.¹⁰

The indentation fracture approach adopted in this and earlier studies¹¹ is a simple means of analyzing and predicting strength-degradation response in a wide range of particle impact situations. In particular, the prospect of obtaining all essential degradation parameters for a given projectile/target system from routine, static Vickers indentation tests, including the residual stress σ_R in tempered surfaces,⁵ remains an attractive feature of the approach.³ With due attention to the possible complications from stress-gradient effects and crack-geometry variants indicated, the analysis should, in principle, be applicable to more complex surface-strengthened ceramic systems than the thermally tempered glass adopted here as a model system.

APPENDIX

Median Crack Initiation in Tempered Surfaces

A model for the initiation of median cracks in untempered surfaces is described in Ref. 6. A simple extension of this model is proposed here to accommodate the effect of a surface compression due to tempering.

The calculation determines the critical conditions necessary to initiate a median crack from a favorably located subsurface flaw in the elastic/plastic indentation stress field. This flaw is idealized as a penny with center at the base of the plastic zone and diameter along the load axis. The peak tensile stress across the crack center scales directly with the hardness, $\sigma_m \propto H$, and accordingly does not change with load. However, the *spatial extent* of the tensile field over the prospective crack area scales with the characteristic dimension of the plastic zone, $b \propto a \propto (P/H)^{1/2}$; in the present model the tensile stress is taken to fall off linearly from the penny center to zero over the radial distance b . It is therefore a critical spatial factor, and not a critical stress, which determines the threshold for median crack initiation.

In a tempered surface a potential median crack nucleus experiences a superposed compressive stress across its area. This extra component is readily incorporated into the model by adding a term in σ_R to the original stress intensity factor for flaws in the indentation field.⁶ In the region of critical behavior,

$$K = 2\sigma_m(c/\pi)^{1/2}(1 - \pi c/4b) - 2\sigma_R(c/\pi)^{1/2} \quad (c \leq b) \quad (A-1)$$

The condition $K = K_c$ for Griffith equilibrium then reduces to

$$1 = C^{1/2}(1 - \pi C/4P^{1/2}) - (\sigma_R/\sigma_m)C^{1/2} \quad (C \leq P^{1/2}) \quad (A-2)$$

where $C \propto (H/K_c)^2 c$ and $P \propto (H^3/K_c^4)P$ are appropriately normalized crack dimension and load, respectively. The minimum (P^*, C^*) in the dimensionless $P(C)$ function corresponds to a lower bound in the initiation requirement; identification of a threshold load P_c with this minimum requirement implies the availability of an optimum flaw of size c^* .⁶ Differentiation of Eq. (A-2) yields

$$P_c = [\alpha_p / (1 - \sigma_R/\sigma_m)^3] K_c^4 / H^3 \quad (A-3)$$

where α_p is a numerical constant. Thus, assuming flaw characteristics to be similar in tempered and untempered surfaces, $P_c(\sigma_R) > P_c(0)$; that is, the effect of surface compression is always to inhibit the initiation of median fracture.

Quantification of Eq. (A-3) requires knowledge of the elastic/plastic indentation field to specify σ_m , and, if absolute values are sought, a suitable calibration of α_p . Taking $\sigma_m \approx 0.1H = 0.6 \text{ GPa}^{12}$

and $\sigma_R \approx 128 \text{ MPa}$ for the tempered glass used here, Eq. (A-3) gives $P_c(\sigma_R) \approx 2P_c(0)$.

Acknowledgment: The writers thank G. Garrett for assistance in collecting the data.

References

- ¹ S. M. Wiederhorn and B. R. Lawn, "Strength Degradation of Glass Impacted with Sharp Particles: I"; this issue, pp. 66-70.
- ² F. M. Ernsberger, "Strength of Brittle Ceramic Materials," *Am. Ceram. Soc. Bull.*, **52** [3] 240-46 (1973).
- ³ D. B. Marshall and B. R. Lawn, "Strength Degradation of Thermally Tempered Glass Plates," *J. Am. Ceram. Soc.*, **61** [1-2] 21-27 (1978).
- ⁴ D. B. Marshall and B. R. Lawn, "Measurement of Nonuniform Distribution of Residual Stresses in Tempered Glass Discs," *Glass Technol.*, **19** [3] 57-58 (1978).

- ⁵ D. B. Marshall and B. R. Lawn, "An Indentation Technique for Measuring Stresses in Tempered Glass Surfaces," *J. Am. Ceram. Soc.*, **60** [1-2] 86-87 (1977).
- ⁶ B. R. Lawn and A. G. Evans, "A Model for Crack Initiation in Elastic/Plastic Indentation Fields," *J. Mater. Sci.*, **12** [11] 2195-99 (1977).
- ⁷ B. R. Lawn and M. V. Swain, "Microfracture Beneath Point Indentations in Brittle Solids" *ibid.*, **10** [1] 113-22 (1975).
- ⁸ S. M. Wiederhorn and D. E. Roberts, "A Technique to Investigate High Temperature Erosion of Refractories," *Am. Ceram. Soc. Bull.*, **55** [2] 185-89 (1976).
- ⁹ B. R. Lawn and D. B. Marshall, "Contact Fracture Resistance of Physically and Chemically Tempered Glass Plates: A Theoretical Model," *Phys. Chem. Glasses*, **18** [1] 7-18 (1977).
- ¹⁰ A. G. Evans and T. R. Wilshaw, "Quasi-Plastic Solid Particle Damage in Brittle Materials: I," *Acta Metall.*, **24**, 939-56 (1976).
- ¹¹ B. R. Lawn and D. B. Marshall, pp. 205-29 in *Fracture Mechanics of Ceramics*, Vol. 3. Edited by R. C. Bradt, D. P. H. Hasselman, and F. F. Lange. Plenum, New York, 1978.
- ¹² R. Hill, *Mathematical Theory of Plasticity*; p. 97. Clarendon, Oxford, England, 1950.